3 Summary

A modified steam-jet agglomerator employing an adjustable system of two oblong, slit-shaped steam nozzles is presented. Nozzle position and steam flow towards the powder curtain were optimized by judging the size of the agglomerates produced. Wetting the feed material, which mainly consisted of dry agglomerates, had to occur with as little turbulence as possible to give best results.

The dry agglomerates, which develop under the influence of ubiquitous attractive forces during feeding, often already possess properties required in instant products while being very fragile. Only thorough wetting and subsequent drying in the steam-jet agglomerator provide the required stability. Here, further size enlargement by agglomeration occurs. The results presented here were mainly derived from experiments with powdered saccharides as main powder component. These materials are fully water-soluble and quickly develop viscous liquid layers when wetted on the surface.

The particle size distribution of the dry agglomerates could be measured for realistic feed rates using an image analysis method. It could be shown that the dry agglomeration was the major size enlargement step. Among other methods, low-pressure roller compaction and vibration feeding were used for feeding and pre-agglomerating the powders. The porosity of the final agglomerates was in a range suitable for instant products at $\varepsilon \approx 0.45$ to 0.6.

Under certain premises, kinematic agglomeration of the particles can be described by a model. Prior to model calculations, the condition for adherence of colliding particles had to be determined by a basic experiment. Discrete population balance simulations were then performed for various operating conditions and step responses to changes in the properties of the feed material were calculated, which confirmed the assumption of a typical start-up time in the order of 2 s. The calculations showed that a wide particle size distribution of the feed material furthers size enlargement by agglomeration. Measurements and calculations of the agglomeration effect were in good agreement.

Acknowledgement

The financial help of the Deutsche Forschungsgemeinschaft (DFG) for this project is gratefully acknowledged.

Received: May 15, 1998 [K 2422]

References

[1] Hogekamp, S., Über eine modifizierte Strahlagglomerationsanlage zur Herstellung schnell dispergierbarer Pulver, Diss., Universität Karlsruhe (TH)/Fakultät für Chemieingenieurwesen 1997.
[2] Buggisch, H., Personal Communication, Karlsruhe, April 21, 1995.
[3] Löffler, F., *Staubabscheiden*, Thieme, Stuttgart 1988.
[4] Kürten, H.; Raasch, J.; Rumpf, H., *Beschleunigung eines kugelförmigen Feststoffteilchens im Strömungsfall konstanter Geschwindigkeit*, in: *Chem. Ing. Tech. 38* (1966) No. 12, pp. 941–948.

This paper was also published in German in Chem.-Ing.-Tech. 71 (1999) No. 3.

Kinetics and Deactivation of the NO Reduction by CO on Pt-Supported Catalysts

By *Brigitta Frank* and *Albert Renken**

Dedicated to Professor Dr.-Ing. Gerhard Emig on the occasion of his 60th birthday

1 Problems

The reduction of NO by CO on Pt has been extensively investigated in the past, since it helps to eliminate NO of the exhaust gas of cars. Despite the stoichiometric simplicity of this reaction, it exhibits many interesting features, such as surface explosions [1], bistabilities and oscillations [2]. On single crystal surfaces it was shown that the dissociation of NO plays an important role in this reaction [3]. However, some authors found that the reaction can be described with a bimolecular mechanism and they deny a possible dissociation of NO [4]. Moreover, some authors observed a deactivation of the NO/CO reaction on Pt-supported catalysts [5,6], of which the origin and the mechanism is not definitely clarified.

In this work, the reduction of NO with CO is examined on a 0.5 % Pt - 3.4 % MoO_3 /α-Al_2O_3 catalyst. The results of a kinetic modeling are presented and a new proposition concerning the mechanism of the observed deactivation is made. To our knowledge, this is the first study where the kinetics of the N_2O formation on a Pt-catalyst is established.

2 Experimental Setup

The experimental setup consists of the gas supply, a loop reactor and an analytic part. Gases are supplied by mass flow controllers without further purification. The reactor consists of a quartz tube (d = 10 mm) containing the catalyst bed and an external circulation loop. The gas mixture is recycled by a membrane compressor (16 l/min). The reactor is heated by a block of stainless steel (l = 140 mm, d = 50 mm), comprising 4 heating cartridges. The temperature in the catalytic bed is measured by a thermocouple movable in a glass capillary. The loop reactor can be considered as an ideal CSTR (continuous stirred tank reactor) [7].

The concentrations of CO_2, N_2O, NO, N_2 and CO are measured by a gas-chromatograph (carrier gas: He, temperature: 60 °C, 2 columns: Porapak S, 1/8, 4.6 m, 80/100 mesh and molecular sieve 5Å, 4 m, 1/4, 60/80 mesh, time of analysis: 52

[*] Dr.-Ing. B. Frank, R&D Fine Chemicals, Lonza AG, CH-3930 Visp; e-mail: brigitta.frank@lonza.ch; Prof. Dr. A. Renken, Laboratory of Chemical Reaction Engineering, Swiss Federal Institute of Technology Lausanne, CH-1015 Lausanne, Switzerland; e-mail: albert.renken@epfl.ch

min). The concentrations of CO_2 and NO are further measured by two infrared detectors. The values are continuously recorded. The temperature is kept at the desired temperature using a PID- controller. The mass flow detectors can be controlled manually or by the computer using D/A converters. During the kinetic measurements an experimental condition is generally kept constant for 4.3 h. The mass balance of N and C of each experimental point is within ± 5 %.

The catalyst containing 0.5 % Pt and 3.4 % Mo is supported on α - Al_2O_3 with a particle diameter of 1 – 1.25 mm. The BET surface is < 3 m^2/g and the average pore size 400 nm. Fresh catalyst is reduced for 2 h at 400 °C with 10 % H_2 in Ar. For the kinetic measurements 0.1 or 0.017 g catalyst are used, which is further treated for 12 h at 450 °C using 2 % NO and 1 % CO.

3 Results and Discussion

The following parallel reactions take place on the Pt-Mo-catalyst:

$$2\,NO + 2\,CO \rightarrow N_2 + 2\,CO_2 \quad (1)$$

$$2\,NO + CO \rightarrow N_2O + CO_2 \quad (2)$$

To establish the kinetics of the system, it is sufficient to model the formation rates of N_2 and N_2O. The other reaction rates can further be calculated by (3) and (4).

$$-R_{NO} = 2\,(R_{N2} + R_{N2O}) \quad (3)$$

$$-R_{CO} = R_{CO2} = 2\,R_{N2} + R_{N2O} \quad (4)$$

The partial pressure of NO is regulated at the outlet of the loop reactor. For a certain partial pressure of NO and temperature, the partial pressure of CO is stepwise increased while maintaining net oxidizing conditions ($p_{CO} < p_{NO}$). The formation rate of N_2 is increasing with increasing partial pressure of CO and with temperature up to a temperature of 455 °C (Fig. 1). However, at 495 °C the formation rate of N_2 is lower than at 455 °C. The apparent reaction order of CO increases from 0.6 at 340 °C to 1 at 495 °C. This is a well-known behavior for Langmuir-Hinshelwood kinetics when interpreting the parameter K_i as equilibrium constant of adsorption: When the adsorption terms are large ($K_i p_i >> 1$) as e.g. at low temperatures, the denominator in (5) is > 1 and the reaction order is < 1. When adsorption terms are small ($K_i p_i << 1$), e.g. at high temperatures, the denominator in (5) is 1 and the reaction becomes first order in i.[1)]

$$R_i = k_i \cdot \theta_{CO} \cdot \theta_{NO} = k_i \frac{K_{NO} p_{NO} \cdot K_{CO} p_{CO}}{(1 + K_{NO} p_{NO} + K_{CO} p_{CO})^2}$$

$$(i = N_2, N_2O) \quad (5)$$

1) List of symbols at the end of the paper.

Hence, the slight decrease of the reaction rate of N_2 at 495 °C can be attributed to the low adsorption constants of CO and NO at this temperature resulting in low coverages.

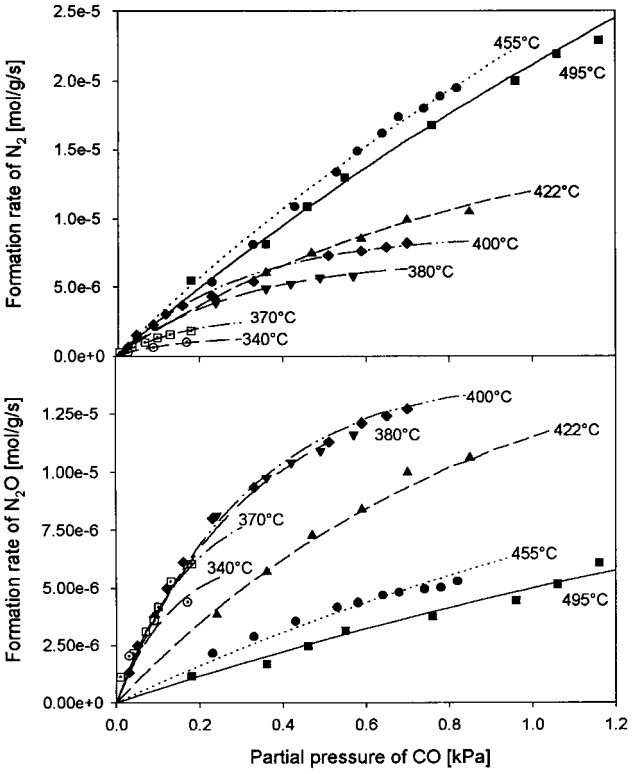

Figure 1. Measured formation rates of N_2 and N_2O at different temperatures (symbols: experimental points) and model (curves) for p_{NO} = 1.6 kPa. Each represented point represents a stationary state.

The reaction rate constant k_i as well as the apparent adsorption equilibrium constants K_i of the used Langmuir-Hinshelwood model (5) are optimized at each temperature (curves in Fig. 1). From the temperature dependence according to Arrhenius (6) and vant Hoff (7) the activation energies $E_{a,i}$ and the adsorption enthalpies ΔH_i are calculated and resumed in Tab. 1.

$$k_i = k_{i0} \cdot \exp(-E_{a,i}/RT) \quad (6)$$

$$K_i = k_{ad,i0}/k_{d,i0} \cdot \exp(-(E_{ad,i} - E_{d,i})/RT) = K_{i0} \cdot \exp(-\Delta H_i/RT) \quad (7)$$

The adsorption enthalpies are 102 kJ/mol for CO and 34 kJ/mol for NO. From the low adsorption enthalpy of NO it can be concluded that the NO dissociation is an activated process. The activation energy for the N_2 formation is 120 kJ/mol. For the N_2O formation an activation energy of 72 kJ/mol is found at temperatures < 400 °C and of 10 kJ/mol at higher temperatures. The formation rate of N_2O cannot be described with an unique reaction rate constant since it already decreases significantly at 400 °C (Fig. 1). Further below a possible origin for this behavior is discussed.

Table 1. Activation energies or adsorption enthalpies and preexponential factors of the Langmuir-Hinshelwood model (5) for the ignited state of the NO/CO reaction.

	$E_{a,i}$ [kJ/mol]		k_{i0} [mol/g/s]		ΔH_i [kJ/mol]		K_{i0} [kPa^{-1}]
k_{N_2}	119	(±9.8)	117039	K_{NO}	-34	(±5.7)	$1.9\cdot10^{-3}$
k_{N_2O}, T < 400°C	72	(±10.)	44	K_{CO}	-102	(±7.)	$1.5\cdot10^{-8}$
k_{N_2O}, T > 400°C	10	(±3.5)	$7.3\cdot10^{-4}$				
k_{CO} [a]	91	(±6.2)	2990				
k_{NO} [a]	78	(±6.0)	369				

[a]: Values were calculated according to Eqs. 3 and 4 .

In Fig. 2 the conversion rate of CO is given as a function of the inlet partial pressure of CO for different NO pressures in a larger range of CO partial pressures. As in the experiments depicted in Fig. 1, p_{CO} was increased in small steps. First the CO conversion rate increases with increasing partial pressure of CO. However, at a critical partial pressure of CO, which depends on the NO partial pressure, the reaction rate decreases suddenly. The next stationary state is only attained at a low reaction rate. The reaction extincts and at higher CO partial pressures the reaction rate rests on a plateau. No stable operation points exist between the ignited and the extinguished state (bistability).

As shown in Fig. 1, in the ignited state the reaction can be described with a bimolecular Langmuir-Hinshelwood model. Nevertheless, this does not signify that the reaction is in effect bimolecular and occurs between adsorbed CO (CO_{ad}) and adsorbed NO (NO_{ad}). The reaction sequence assuming a dissociative mechanism is summarized in (8–13). Herein, the dissociation of NO_{ad} occurs before the reaction with CO_{ad}.

$$CO + Z \rightleftarrows CO_{ad} \quad (8)$$

$$NO + Z \rightleftarrows NO_{ad} \quad (9)$$

$$NO_{ad} + Z \rightarrow N_{ad} + O_{ad} \quad (10)$$

$$CO_{ad} + O_{ad} \rightarrow CO_2 + 2\,Z \quad (11)$$

$$N_{ad} + N_{ad} \rightarrow N_2 + 2\,Z \quad (12)$$

$$N_{ad} + NO_{ad} \rightarrow N_2O + 2\,Z \quad (13)$$

The bistabilities displayed in Fig. 2 can only be caused by a dissociative mechanism, not by a bimolecular mechanism. A bimolecular mechanism would lead to a slow decrease of the reaction rate, but not to an abrupt extinction as in Fig. 2. Furthermore, a bimolecular expression as in (5) can result from a dissociative mechanism (8–13), when the dissociation of adsorbed NO (10) is much faster than the reaction of the dissociation products N_{ad} and O_{ad} (11–13). Moreover, the observed decrease of the N_2O formation at 400 °C can only be explained by a dissociative, but not with a bimolecular mechanism: When N_2O is formed by $NO_{ad} + N_{ad}$ (13) and N_2 by $N_{ad} + N_{ad}$ (12) [8], only the formation of N_2O is impeded when the NO dissociation is complete. Hence, it is possible that only the formation rate of N_2O but not the formation rates of N_2 and CO_2 decrease above 400 °C.

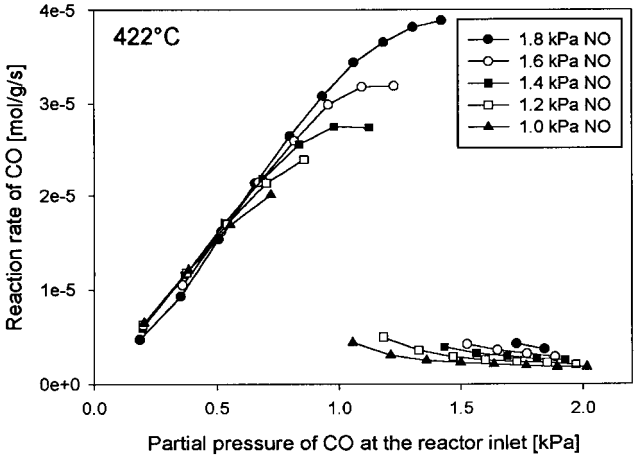

Figure 2. Bistability of the NO/CO reaction for different partial pressures of NO as a function of the inlet partial pressure of CO. Each represented point represents a stationary state.

If reducing conditions ($p_{CO} >> p_{NO}$) were employed when the catalyst was kept for 60 h under argon, the conversion of CO as well as of NO decreased slowly with time, starting at high conversions: the catalyst deactivates. The conversion of NO decreases in 12 hours from 90 to 60 % and a stationary state is still not obtained (Fig. 3, I). After keeping the catalyst once more for 12 h under argon, the NO conversion is again 90 % and decreases slowly to 60 % (Fig. 3, II). The deactivation is therefore reversible. Under oxidizing conditions ($p_{CO} < p_{NO}$) a stationary state is already attained after 2 h (Fig. 3, III). Since the catalyst can be activated under an inert gas, the deactivation cannot be due to a deposition of carbon, which would be irreversible. An influence of molybdenum oxide as oxygen-storage device can also be excluded, as the deactivation is also found on a Pt/α–Al_2O_3 catalyst (Fig. 4). The results therefore suggest that the deactivation is due to adsorbed species, desorbing under argon.

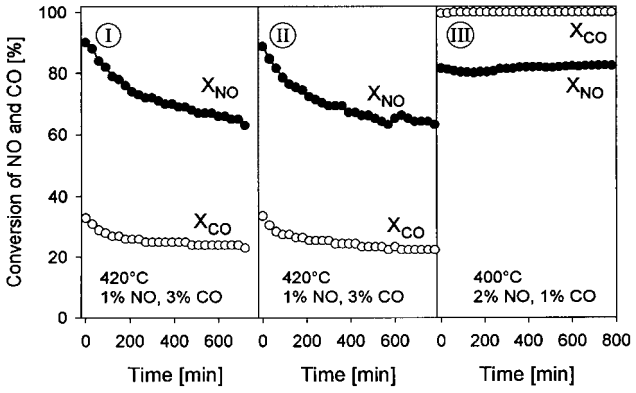

Figure 3. I, II: Reversible deactivation of the NO/CO reaction under net reducing conditions. III: Stationary state under net oxidizing conditions. Each represented point represents a measurement.

Two other groups also reported of a reversible deactivation of the NO + CO reaction [5,6]. Both groups noticed that the deactivation is independent of the previous treatment of the catalyst. Lorimer and Bell [5] found a deactivation on a Pt/

SiO_2 catalyst and observed the formation of a strong isocyanate (-NCO) peak in the infrared spectrum. They propose that isocyanates are responsible for the deactivation. Mergler and Nieuwenhuys [6] found a deactivation on a Pt/Al_2O_3 catalyst. As they did not find the typical peak for isocyanates at 2180 cm^{-1} (Pt-NCO), they assume that a strongly adsorbed Pt^{n+}-CO species with a peak at 2120 cm^{-1} causes the deactivation. Such a species is observed by some authors during the CO + O_2 reaction [9].

To clarify whether a Pt^{n+}-CO or a Pt-NCO species is responsible for the deactivation, a fresh catalyst (0.5 % Pt/α-Al_2O_3) is pretreated and a reducing mixture of CO/O_2 is introduced into the reactor. After some hours, the reactor is purged with argon and a reducing CO/NO mixture is introduced. The results are resumed in Fig. 4: For the CO + O_2 reaction a stationary state is attained after one hour. For the CO + NO reaction a slow deactivation is again found and a stationary state is only obtained after 10 h. These results clearly indicate that a Pt^{n+}-CO species which should also be formed during the CO + O_2 reaction cannot be responsible for the deactivation. The deactivation must therefore be caused by an N-containing species as isocyanates (-NCO) or cyanates (-CN).

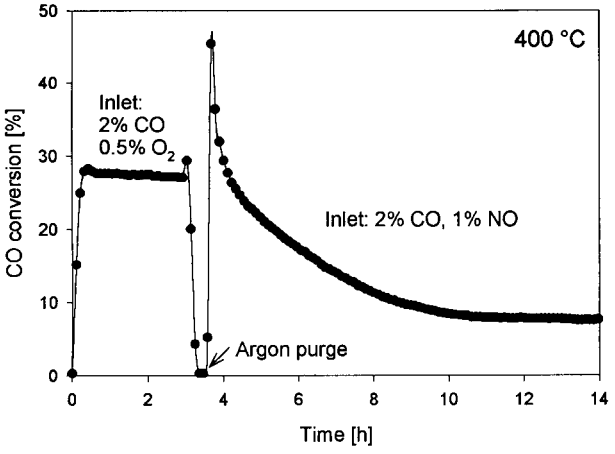

Figure 4. Comparison of the CO/O_2 and the NO/CO reaction under reducing conditions on a 0.5 wt.-% Pt catalyst supported on α–Al_2O_3. Each represented point represents a measurement.

The fact that Mergler and Nieuwenhuys did not find a peak at 2180 cm^{-1} might be due to the low stability of Pt-NCO species [10]. It was shown that isocyanates form solely on the metal and that they later diffuse on to the support, where they rest [11].

At this point, a possible deactivation mechanism should be discussed on a molecular level. Lorimer and Bell [5] suggest that the formed isocyanates reduce the electron density of Pt and thus restrain the dissociation of NO. They further believe that this causes the observed deactivation of the catalyst. In contrast to this, it is proposed in the present paper that the formation of the isocyanates is not a deactivating, but rather an activating process:

At the experimental conditions where the deactivation is found here (2 % CO, 1 % NO or 0.5 % O_2) the reaction is extinguished. In the experiment depicted in Fig. 4 this state is certainly attained very slowly. By contrast, in the CO + O_2 reaction the extinguished state is attained somewhat faster. Hence, the observed deactivation is rather a slow attainment of the extinguished state. In the extinguished state, the dissociation of NO and thus the reaction is inhibited by high concentrations of strongly adsorbed CO [12], not by isocyanates. After their formation on Pt, isocyanates are found to migrate on the support, where they remain without altering the reaction any more [11]. However, the slow formation of the isocyanates delays the development of the strong Pt→CO bond and consequently the dissociation of NO can take place for a longer time. This delay might occur by lowering the electron density of Pt, as proposed by Lorimer and Bell [5], since a low electron density of Pt decreases the strength of the Pt→CO bond. Since the reaction rests longer in the ignited state and the extinction is delayed by the formation of the isocyanates, isocyanates have rather an activating and not a deactivating effect.

As a result, it should be possible to attain the extinguished state faster when increasing the CO concentration in small steps. This permits the migration of the isocyanates on the support. This approach was successfully used in the experiment shown in Fig. 2, where the extinguished state was attained after 1–2 hours.

4 Conclusions and Perspectives

The NO + CO reaction shows an ignition/extinction behavior on a 0.5 % Pt/3.4 % MoO_3 /α-Al_2O_3 catalyst using a loop reactor. In the ignited state the reaction rates can be described by a bimolecular Langmuir-Hinshelwood model. This is in agreement with a dissociative mechanism, when the dissociation of NO is sufficiently fast.

In contrast to the CO + O_2 reaction a slow deactivation is observed for the NO + CO reaction when switching suddenly to net-reducing conditions with $p_{CO} >> p_{NO}$. It is proposed that the slow formation of isocyanates reduces the electron density of Pt and that this delays the formation of the strong Pt→CO bond dominating in the extinguished state. The presented mechanism differs fundamentally from the mechanisms proposed by other authors [5,6]. Both groups suggest that a strongly adsorbed species (Pt-NCO or Pt^{n+}-CO) is responsible for the deactivation and thus for the low activity in the extinguished state. In contrast to this it is proposed here that the formation of the isocyanates only delays the attainment of the extinguished state, but that the low activity in the extinguished state is due to strongly adsorbed CO and not to the presence of isocyanates.

Acknowledgment

Financial support by the Swiss National Science Foundation is gratefully acknowledged. Prof. Dr.-Ing. G. Emig is acknowledged for helpful discussions.

Received: July 30, 1998 [K 2454]

Symbols used

$E_{a,i}$	[kJ/mol]	activation energy
ΔH_i	[kJ/mol]	adsorption enthalpy of species i
$k_{ad,i}$	[-]	adsorption constant of species i
$k_{d,i}$	[-]	desorption constant of species i
k_{i0}	[mol/g/s]	preexponential factor
K_i	[-]	equilibrium constant of adsorption of species i
p_i	[kPas]	partial pressure of species i
R_i	[mol/g/s]	reaction rate of species i
Z	[-]	free surface site
θ_i	[-]	surface coverage of species i

References

[1] Fink, T.; Dath, J.-P.; Bassett, M. R.; Imbihl, R.; Ertl, G., *Surf. Sci. 245* (1991) pp. 96–110.
[2] Frank, B.; Doepper, R.; Emig, G.; Renken, A., *Catal. Today 38* (1997) pp. 59–69.
[3] Banse, B. A.; Wickham, D. T.; Koel, B. E., *J. Catal. 119* (1989) pp. 238–248.
[4] Scharpf, E. W.; Benzinger, J. B., *J. Catal. 136* (1992) pp. 342-360.
[5] Lorimer, D. A.; Bell, A. T., *J. Catal. 59* (1979) pp. 223-238.
[6] Mergler, Y. J.; Nieuwenhuys, B. E., *J. Catal. 161* (1996) pp. 292–303.
[7] Frank, B., Ph. D. Thesis, Swiss Federal Institute of Technology, Lausanne 1997.
[8] Burch, R.; Millington, P. J.; Walker, A. P., *Appl. Catal. B 4* (1994) pp. 65–94.
[9] Barshad, Y.; Zhou, X.; Gulari, E. J., *Catal. 94* (1985) pp. 128–141.
[10] Rasko, J.; Solymosi, F. J., *Catal. 71* (1981) pp. 219–222.
[11] Solymosi, F.; Völgyesi, L.; Sarkany, J. J., *Catal. 54* (1975) pp. 336–344.
[12] Muraki, H.; Fujitani, Y., *Ind. Eng. Chem. Prod. Res. Dev. 25* (1986) pp. 414-419.

This paper was also published in German in Chem.-Ing.-Tech. 71 (1999) No. 1+2.

Hydrolysis of Nitriles in Supercritical Water*

By *Alexander Krämer, Sabine Mittelstädt* and *Herbert Vogel***

1 Introduction

Water plays an important role in many chemical reactions: as a solvent, a reaction partner or a catalyst. It is inexpensive, nontoxic, it is neither inflammable nor explosive and it is ecologically safe. At high temperatures water tends to be an extremely reactive partner. The properties of the aqueous reaction mixture, especially near the critical point, can be controlled through minor temperature and pressure variations and they can be adapted to the chemistry without having to find an alternative solvent to water.

In order to investigate the synthesis potential of hot water in near- and supercritical conditions, the conversion of acetonitrile and benzonitrile (representing aliphatic and aromatic nitriles, respectively) was examined in near- and supercritical water in the temperature and pressure ranges of 300–450 °C and 23–32 MPa, respectively.

Up to now, the hydrolysis of acetamide [1], isobutyronitrile [2,3,4], benzonitrile [3,4], benzamide [5] and butyronitrile [6] has only been examined under subcritical conditions. In most of these published papers, either very small batch autoclaves or tubular reactors were used in the examinations and therefore in this kind of apparatus catalytic wall effects cannot always be safely excluded. The following investigations of the synthesis potential of hot water at sub- and supercritical conditions were carried out in a continuous plant with technical dimensions.

2 Experimental

2.1 Testing Plant

The principal item of the continuous high-pressure apparatus is a tubular reactor made of Inconel 625, which measures one meter in length and has a capacity of 50 ml. The maximum possible working conditions of this apparatus are 50 MPa and 500 °C, with residence times between 6 and 400 s. The water-soluble educts (acetonitrile and acetamide) were fed directly into the reactor whereas the water-insoluble educts (benzonitrile) were fed into the reactor via two separate high-pressure pumps. A detailed description of the high-pressure plant is given elsewhere [7].

[*] Lecture given by A. Kramer at the GVC Fachausschußsitzung Reaktionstechnik in Aachen, Germany, on March 4, 1998.

[**] Dipl.-Ing. A. Krämer, Dr.-Ing. S. Mittelstädt, Prof. Dr.-Ing. H. Vogel (author to whom correspondence should be addressed), Darmstadt University of Technology, Department of Chemistry, Institute of Chemical Technology, Petersenstr. 20, D-64287 Darmstadt, Germany.

  0930-7516/99/0606-0494 $ 17.50+.50/0